Investigating the mechanism of influenza infection inhibition of alveolar epithelial cells by alveolar macrophage-derived extracellular vesicles

Katherine Smith
Honors Thesis
Department of Molecular, Cellular, and Developmental Biology
University of Michigan - Ann Arbor, MI

ACKNOWLEDGEMENTS

ABSTRACT

Influenza infection of distal airways in human lungs is linked to an increased risk of death. Intercellular communication between resident alveolar epithelial cells (AECs) and alveolar macrophages (AMs) plays an essential role in the body's innate defense against inhaled pathogens. Extracellular vesicles (EVs) are small, double membrane-bound packages of proteins, lipids, and RNAs secreted by nearly all cell types. They modulate physiologic functions in a variety of contexts. AM-derived EV (AM-EV) communication is an emerging example of intercellular communication at this site but has not been explored in the context of host defense against influenza. Unpublished background data prompting the studies in this thesis demonstrate that uptake of AM-EVs protect AECs against influenza infection at an early, intracellular stage of the viral replication cycle. This activity of AM-EVs was present against only a subset of influenza strains studied and depended on the specific hemagglutinin expressed by the strain. The early, intracellular stage of the influenza replication cycle mediated by hemagglutinin is endosomal fusion. Therefore, we hypothesized that AM-EVs inhibit the endosomal fusion of susceptible influenza strains, preventing their translocation into and replication within the nucleus. To test this, we performed confocal immunofluorescence studies to evaluate the effect of AM-EVs on the localization of differentially-inhibited influenza strains to late (acidified) endosomes. Furthermore, in these strains, we characterized their relative sensitivity to endosomal acidification inhibitors and established the kinetics of their escape from late endosomes. In sensitive strains, AM-EVs inhibit influenza infection in AECs at the point of viral-endosomal fusion, trapping the virus in late (acidified) endosomes. Additionally, sensitive strains escape the endosome earlier, suggesting that the pH of viral-endosomal fusion of susceptible strains is higher than that of resistant strains. These results suggest that AM-EVs drive endosomal pH to an acidic range facilitating fusion of resistant strains, but outside the optimal fusion pH range of susceptible strains. By defining the stage of infection targeted by AM-EVs, this will inform future studies toward the identification of responsible mediators within EVs as well as efforts to improve antiviral therapies.

INTRODUCTION

Alveoli are the thin-walled, sac-like structures located in the distal airways of the lung. Their primary function is to exchange gases between the bloodstream and air inhaled into the alveolar space. The microenvironment of these distal air spaces is one plagued with homeostatic challenges for their resident cell types. Routinely exposed to airborne antigens and infectious diseases such as influenza, the niche of cells at this site must combat these threats while prohibiting an inflammatory response great enough to be detrimental to their function.

Influenza is a potentially life-threatening virus that infects the respiratory tract of several mammalian species, including humans. In the 2017-2018 season alone, 61,000 people died as a consequence of influenza, worldwide Centers for Disease Control and Prevention Foundation [CDC], 2019). Influenza causes great strife in both the health care and research communities due to the morbidity and mortality associated with this infection. Influenza-associated costs to the US alone total nearly 100 billion dollars annually (CDC, 2014). There are currently 4 types of influenza that have been classified: Influenza A (IAV), B, C, and D Virus. IAVs are of primary concern to health care providers and researchers, as 75% of influenza cases are caused by IAVs (Nyirenda et al., 2016). IAVs primarily infect the cells residing in the large, or proximal, airways (CDC, 2017). However, infection may progress to the smaller, distal airways of the lung and lead to infection of the alveoli. It is infection at this site that is associated with an increased risk of death (Oslund et al., 2011). Here, we study a mechanism by which resident innate immune cells combat an influenza infection at this vital site.

Alveolar macrophages (AMs) are the primary phagocytic cell type at this site and are known to initiate inflammatory responses in alveoli (Peters-Golden, 2004; Rubins, 2003). Resident AMs possess several protective innate immune functions in the alveolar space, such as clearance of microbes (Peters-Golden, 2004). In the context of influenza infection, AMs have been shown to play an important role in host defense through various means: 1) AMs infected with influenza secrete pro-inflammatory cytokines in order to combat the infection (Seo et al., 2004); 2) AMs ingest apoptotic bodies created by a productive influenza infection (Duan et al., 2017); and 3) AMs sequester influenza virions without enabling productive replication in themselves (Duan et al., 2017). However, despite being one of two primary cell types in the alveolar space and the resident innate immune cell at this site, recent studies have shown that there is only one AM per 3 alveoli (Bhattacharya et al., 2016). Additionally, AMs have been shown to be relatively immobile in vivo (Westphalen et al., 2014). These findings suggest a necessity for AMs to use paracrine signaling to maintain homeostasis at this site; however, AM paracrine signaling in the context of influenza infection has yet to be explored.

One form of paracrine signaling which AMs utilize that has recently gained momentum in the research community is mediated by extracellular vesicles (EVs). EVs are small (<1μm), double membrane-bound compartments originating from endosomal or plasma membranes and secreted by all cell types (Margolis and Sadovsky, 2019). Several

subtypes of EVs have been defined based primarily on size; exosomes (50-100nm vesicles derived from multivesicular bodies), microparticles (200nm-1μm vesicles resulting from plasma membrane budding), and apoptotic bodies (formed from membrane disintegration) are considered three of the main EV classifications (Margolis and Sadovsky, 2019). Originally thought to solely be a means of excreting unnecessary molecules from the parent cell (Margolis and Sadovsky, 2019), it is now known that EVs transport functional proteins, nucleic acids, and lipids to adjacent or distant cells (Margolis and Sadovsky, 2019). EVs are used to communicate with and able to alter the physiology of recipient cells (Margolis and Sadovsky, 2019). In the distal airways, specifically, EVs isolated from AMs (AM-EVs) play an important role in maintaining homeostasis. As Speth et al. demonstrated, AM-EV packaging of a cytokine suppressor (SOCS3) is influenced by the presence of bioactive mediators that create an environment that mimics acute lung injury (2016). Additionally, Schneider et al. demonstrated that AECs control their uptake of AM-EVs in response to environmental factors (2017). The controlled packaging and uptake of AM-EVs make them ideal particles for modulating the host's response to viral infections.

Notably, the role of EVs in the spread of disease pathology and viral infection is a double-edged sword (Rubins, 2003). Several studies have implicated this form of intercellular communication in mediating the spread of many diseases and infections (Meckes and Raab-Traub, 2011; Asai et al., 2015; Rudnick et al., 2017). During viral infections, specifically, EVs can favor the host or the virus. In some infections, EVs released from infected cells have been shown to carry viral and/or host factors that ultimately facilitate productive infection of the recipient cell (Madison et al., 2015; Liu et al., 2014; Fu et al., 2017) or induce apoptosis in uninfected cells (Lenassi et al., 2010). Conversely, several studies have demonstrated a protective role of EVs against viral infections such as influenza. EVs derived from AECs are able to deliver functional host and viral cargo, inducing interferon production in recipient AECs and subsequently inhibiting influenza infection (Liu et al., 2019). Additionally, EVs isolated from bronchoalveolar lavage fluid were recently shown to differentially express several microRNAs and, consequently, upregulate pro-inflammatory cytokines during influenza infection (Maemura et al., 2018). Despite the evidence that EVs play a role in host immune responses and the apparent necessity for AM paracrine signaling to mediate pro- and anti-inflammatory responses at this site, nothing is known about the explicit role of AM-EVs in the host's response to influenza.

To better understand AM paracrine signaling in host response to influenza infection of alveoli, our lab investigated the role of AM-EVs (which we will simply refer to as "EVs" for the rest of this paper for the sake of simplicity) in the context of influenza infection of AECs. Our lab (Schneider et al., unpublished data) found that:
- Secreted mediators from AMs inhibit influenza infection of epithelial cells, and this inhibitory activity localizes to EVs.
- EVs isolated from mouse AMs and human macrophages also demonstrate this inhibitory effect against influenza infection.
- EVs inhibit influenza infection of both canine kidney epithelial (MDCK) cells – the classical cell line used in influenza research – and AECs.

- EVs inhibit influenza infection in AECs in vitro and in vivo.

The lab further characterized the mechanism by which EVs inhibit influenza infection of AECs and found that:

- Influenza infection is inhibited by EVs at an intracellular stage.
- Inhibition of influenza infection by EVs does not occur within 1 hour of infection of epithelial cells, but consistently occurs within 3 hours of infection, thus providing data regarding the timing of inhibition in reference to a single replication cycle of influenza (~6 hours, total).
- The inhibitory activity of EVs depends on the subtypes of the viral surface proteins hemagglutinin (HA) and neuraminidase (NA) expressed by the influenza strain.

The goal of the studies in this thesis were to 1) validate Schneider et al.'s unpublished findings regarding HA-/NA-specific differential strain sensitivity to EVs; 2) identify the stage of viral replication targeted by EVs; and 3) identify a means of their inhibitory activity.

By identifying the stage of replication targeted by EVs, we anticipated being in a better position to identify the mechanism of inhibition of influenza by EVs. Notably, the proteins HA and NA are essential to several stages of the viral replication cycle and are major determinants of IAV infectivity, transmissibility, and pathogenicity (Sakai et al., 2017). While several HA and NA isotypes exist, H1N1 and H3N2 combinations are endemic culprits for both seasonal (similar, recurring strains against which most people have some immunity built) and pandemic (new strains that arise from mutations against which most people have no built immunity) influenza in the human population (Dou et al., 2018). As such, these strains of IAV were of primary concern to our research efforts.

NAs are enzymes capable of cleaving sialic acid, a sugar located on the terminal ends of many glycoproteins and glycolipids (Cohen et al., 2013; Yang et al., 2014). These glycoproteins and glycolipids coat cell surfaces and reside within mucus membranes (Cohen et al., 2013; Yang et al., 2014). HA is a protein that binds to receptors on cell surfaces of mucus membranes within the upper respiratory tract via interaction with the terminal sialic acids of these viral-receiving glycoproteins (Sakai et al., 2017). The combined functions of HA and NA are, therefore, essential in mediating viral progression through mucus membranes in order to reach and bind to target cells. While HA is known to mediate viral entry into the target cell through receptor-mediated endocytosis, Schneider et al. was able to eliminate the possibility of EVs preventing viral surface binding as the mode of viral inhibition (unpublished data), urging us to look at a later HA-/NA-dependent stage in the replication cycle. Upon internalization, the virion enters and is trafficked through the cell within an endosome - a small, membrane-bound compartment of the cell that originates from intracellular budding of the plasma membrane. Endosomes move inwards from the cell periphery and undergo a regulated process of gradual acidification during this journey to a late (acidified) endosome in order to prepare to merge with their ultimate destination: the lysosome (Elkin et al., 2016). However, before the virion-containing endosome reaches the lysosome, the low pH of the late endosome induces a conformational change in HA. This change enables fusion of the viral envelope with the endosomal membrane and, consequently, enables

release of the influenza RNA into the cytoplasm. The viral RNA then translocates into the nucleus and hijacks host cell transcription and translation machinery to assemble new viral molecules. These viral molecules assemble at the intracellular surface and bud from the plasma membrane in a NA-dependent manner (Shtyrya et al., 2009). Newly-released viral clones then repeat the cycle, locating and infecting other cells. The time necessary to complete one full replication cycle from the time of entry to production of new virus varies slightly among strains, but usually only takes about 6 hours (World Health Organization [WHO], 2020). Given that the replication cycle of influenza is about 6 hours, Schneider et al.'s finding that EVs inhibit influenza within 3 hours of infection (unpublished data) suggested that the stage of influenza inhibited by EVs is before plasma membrane budding of new viral molecules. With the additional knowledge that EVs inhibit influenza at an HA- or NA-dependent stage of the replication cycle (Schneider et al., unpublished data), we hypothesized that EVs inhibit fusion of susceptible strains with the endosomal membrane early in infection. Under the assumption that EVs inhibit viral-endosomal fusion, we hypothesized that EVs did so via manipulation of endosomal pH, given the pH-dependent conformational change required in HA for influenza to progress beyond this stage of the replication cycle.

To test these hypotheses, we first confirmed that the antiviral effect of EVs is solely due to variances in HA or NA using reassortant viral strains. To understand the role of EVs on influenza at the point of viral-endosomal fusion, we performed confocal immunofluorescence studies to evaluate the colocalization of influenza nucleoprotein (NP) with the late endosomal marker Rab-7. Finally, we performed endosomal acidification inhibitor assays and timed endosomal escape assays using the acidification inhibitors bafilomycin and/or chloroquine to distinguish strain differences in the pH of viral-endosomal fusion. We found that EVs inhibit influenza replication in AECs at the point of viral-endosomal fusion, trapping the virus in late (acidified) endosomes. Our studies suggested that EVs likely inhibit this stage of viral replication by reducing endosomal pH to a point beyond which susceptible strains are not able to fuse with the endosomal membrane. By identifying the stage of replication targeted by EVs and their mode of inhibition at this stage, we hope to inform the identification of responsible mediators within EVs as well as efforts to improve antiviral therapies.

MATERIALS AND METHODS

Statistical Analysis and Data Presentation
Statistical analysis was performed between means of condition replicates unless otherwise noted. Experiments were performed in triplicates unless otherwise noted. Data analysis was performed using GraphPad Prism 8.0 software and utilized One-way ANOVA with Turkey's multiple comparison post hoc analysis or Student's t-test where appropriate. All individual data points within each condition is displayed in figures for transparency. Statistical significant was set at $p < 0.05$. The following symbols were used to display p value ranges: * $p \leq 0.05$, ** $p \leq 0.01$, *** $p \leq 0.001$, **** $p \leq 0.0001$.

Reagents, Cell Lines, and Culture Medium

MDCK cells (ATCC) were cultured in DMEM (Gibco) supplemented with 10% FBS and penicillin/streptomycin (Invitrogen) unless otherwise noted. A549 adenocarcinoma human alveolar basal epithelial cells (ATCC) and MH-S AMs (ATCC) were cultured in RPMI 1640 without L-glutamine (GIBCO) supplemented with 10% FBS and penicillin/streptomycin (Invitrogen) unless otherwise noted. Viral infections occurred in viral growth medium (VGM): DMEM supplemented with 2mg/mL TPCK-treated trypsin (Sigma); 25mM HEPES (GIBCO Cat. #15630); 0.1875% BSA (Sigma); and penicillin/streptomycin (Invitrogen). Acidification inhibitors bafilomycin (B 1793) and chloroquine (C6629-25G) were purchased from Sigma. Bafilomycin was reconstituted in 100% DMSO and stored in -80°C. Working dilutions of bafilomycin and corresponding controls were diluted to 0.1% DMSO in cell culture medium. Chloroquine was reconstituted in sterile water and stored in -80°C.

Viruses

A nanoluciferase was previously cloned downstream of the segment of the influenza genome encoding the polymerase acidic (PA) protein to create the luciferase-expressing (Luc-) WSN/33 strain (Tran et al., 2013). Luc-WSN/33 was demonstrated to be equally as virulent as wild-type (WT) WSN/33; competently replicate within the same host range as WT WSN/33; and have high specific activity (light output) (Tran et al., 2013). WT viruses were obtained from the sources listed in Table 1. Using standard reverse genetics (Hoffman et al., 2002), Luc-strains were generated from these WT strains prior to my thesis work. The influenza A genome consists of 8 negative-sense, single-stranded RNA segments, one of which encodes the HA protein and another encodes the NA protein. To create the reassortant, Luc-expressing strains, plasmids encoding the HA and NA gene segments from WT strains were generated and combined with plasmids encoding the remaining 6 influenza genome segments originating from Luc-WSN/33 (including the Luc-PA segment). Titers of the resulting reassortant strains were determined using the TCID/50 method.

Table 1: Viral Strain Sources

WT Virus Strain	Abbreviation	Source
Influenza A/WSN/33 (H1N1)	WSN/33	ATCC
Influenza A/Wyoming/3/2003 (H3N2)	WY/03	Dr. Arnold S. Monto; University of Michigan School of Public Health
Influenza A/Ann Arbor/2017 (H3N2)	AA/17	Dr. Arnold S. Monto; University of Michigan School of Public Health
Influenza A/Hong Kong/4801/2014 (H3N2)	HK/14	Centers for Disease Control and Prevention International Reagent Resource

Influenza A/Singapore/INFIMH-16-0019/2016 (H3N2)	Sing/16	Centers for Disease Control and Prevention International Reagent Resource
Influenza A/Wisconsin/67/2005 (H3N2)	WI/05	Centers for Disease Control and Prevention International Reagent Resource
Influenza A/California/07/2009 (H1N1)	CA/09	Centers for Disease Control and Prevention International Reagent Resource

Extracellular Vesicle Isolation and Quantification

Mouse MHS AMs (ATCC) were plated on polystyrene flasks and grown to confluency in RPMI 1640 culture medium containing 10% FBS and penicillin/streptomycin. Once confluent, cells were lifted with trypsin 0.25%, pelleted using centrifugation (250 g for 5 min) at 4 °C, resuspended in serum-free RPMI, plated onto fresh flasks, and incubated overnight. The resulting conditioned media was collected and depleted of cell debris and apoptotic bodies via serial centrifugation (500 g for 5 min followed by 2500 g for 12 min) at 4°C. EVs were pelleted using ultracentrifugation (17,500 g for 30 min) at 4°C (Bourdonnay et al., 2015). The pelleted EVs were washed with PBS and pelleted again using ultracentrifugation (17,500 g for 30 min). The pelleted EVs were resuspended in PBS and aliquoted. EV concentration was quantified for each isolation using flow cytometry. EVs were identified and quantified by comparative size to calibration beads. EV concentration was determined by analysis using FlowJo software (*FlowJo, LLC*).

Luciferase Assays for Real-time Quantification of Viral Replication

To assay viral replication in Luc-expressing influenza strains (Luc-strain), for all luciferase assays, MDCKs were seeded at 90% confluency on flat-bottom 96-well plates in serum-containing medium overnight. Cells were then washed; infected with the appropriate reassortant strain; and provided Enduren luciferase substrate (Promega E6481) according to manufacturer's instructions, with or without EVs or inhibitors diluted in VGM. Luminescence was read and recorded from each well at 90 second intervals using a Synergy H1 Luminescence Reader (BioTek) with CO_2 regulator (BioTek) plate reader. Cells were kept at 37°C and 5% CO_2 concentration during readouts. Readouts were taken until the first condition reached the end of the viral exponential growth phase (16-24 hours for all experiments) unless otherwise noted. All experiments were performed with a multiplicity of infection (MOI) of 1 unless otherwise noted.

Viral replication luciferase data is presented as measurements of luminescence area under the curve (AUC) values. The AUC value represents the sum total of viral replication in a set period of time. AUC values were normalized to the control and averaged for each condition. Statistical analysis was performed between means of condition replicates unless otherwise noted.

Acidification Inhibitor IC50 Assay

MDCK cells were pre-incubated for 30 min with the indicated concentrations of bafilomycin or chloroquine. Cells were subsequently co-incubated in VGM with the indicated Luc-strain, the same concentration of acidification inhibitor, and substrate. For a given 96-well plate, 4 strains with each dose of inhibitor were performed as triplicates. For these experiments, nonlinear regression was performed on AUC values and IC50 curves were calculated and generated for each condition using Prism 8 software.

Endosomal Escape Assay

MDCK cells were cooled on ice for 30 min, washed with ice-cold PBS, and incubated with the indicated Luc-stain diluted in VGM on ice for 45 min to allow virions to bind without being internalized. Cells were then washed with cold PBS to remove unbound virus. Cells were incubated with substrate in VGM at 37°C and 5% CO_2 to initiate viral internalization. Bafilomycin was added to a final concentration of 10nM at the indicated time points, which refer to the duration of the incubation at 37°C and 5% CO_2 prior to bafilomycin addition. Upon the final timed addition of bafilomcyin (80 min), cells were placed in the luminescence reader as described above. Replication was determined by luminescence measurements taken over the course of a total of 6 hours of infection time at 37°C, so as to limit the assay to one replication cycle (World Health Organization [WHO], 2020).

Immunofluorescence Microscopy

Human A549 AECs were plated overnight at a density of 1.1e5 cells per well on fibronectin (Sigma; 1.25ug/cm2)-coated number 1.5 coverglass chamber slides (Lab-Tek, Nunc) in RPMI supplemented with 5% FBS and streptomycin/penicillin. Cells were washed and co-incubated for 40 min with virus with EVs or PBS control in VGM. WSN/33 and HK/14 virus was given at a MOI of 1. Cells were washed with PBS, fixed with 4% paraformaldehyde in PBS (10 min @ RT), permeabilized with 0.1% Triton X-100 (5 min @ RT), followed by an incubation in block solution (0.3M glycine, 2% BSA, and 5% goat serum) (45 min @ RT). Primary staining was performed as sequential overnight incubations at 4°C using rabbit anti-Rab7 for late endosomes (Cell Signaling Technologies, 9367) (1:100) followed by mouse anti-influenza NP (Abcam, ab20343) (2.89 ug/mL), in block solution. Secondary staining was performed sequentially and according to manufacturer specifications with Alexa Fluor 488 anti-mouse IgG (1:1000) followed by Alexa Fluor 568 anti-rabbit IgG (1:1000). Cells were covered with DAPI Prolong Gold mounting medium (Invitrogen). Images were taken from an SP5X inverted confocal microscope and analyzed with Application Suite Advanced Fluorescence Software (Leica). Images were captured with laser intensities and amplifier gains set to avoid pixel saturation. Fluorophores were independently excited and detected sequentially. Individual images were captured at a 100 objective with 1.4 numerical aperture, oil immersion, and pinhole set to 1 µm. Z stack images were captured at 512x512 pixel resolution and were subsequently visualized and created with ImageJ software (National Institutes of Health). Virus nuclear localization was quantified as a ratio of NP intensity within the DAPI region divided by total cellular NP intensity.

Colocalization of influenza within late endosomes was quantified as the M2 colocalization coefficient of NP and Rab-7 staining using the coloc 2 plugin in ImageJ.

RESULTS

Patient-derived, luciferase-expressing influenza strains are differentially sensitive to EVs in a HA-/NA-dependent manner

WSN/33 is the quintessential lab-adapted influenza strain used for research studies. Initial unpublished findings of Schneider et al. used a WSN/33 strain previously constructed to express a luciferase reporter gene (Tran et al., 2013). This Luc-strain generates luminescence within infected cells with high specific activity and provides a time-integrated, high-throughput readout of competent viral replication. However, WSN/33 (and Luc-WSN/33) cannot infect humans or wild mice (Staeheli et al., 1988, Thangavel and Bouvier, 2014), and its mechanism of infection is unique from that of strains circulating in the human population (Goto et al., 1998). While both WT and Luc-WSN/33 were demonstrated to be sensitive to inhibition by EVs in AECs via RT-qPCR and luciferase assays, respectively (Schneider et al., unpublished), it was therefore necessary to confirm the activity of EVs against clinically-relevant, patient-derived strains.

Using standard reverse genetics (Hoffman et al., 2002), luciferase-expressing seasonal HK/14 and pandemic CA/09 strains were generated from primary isolates of these influenza strains. As described in Materials and Methods, the influenza A genome consists of 8 negative-sense, single-stranded RNA segments, one of which encodes the HA protein and another encodes the NA protein. Plasmids encoding the HA and NA gene segments from WT strains were generated and combined with plasmids composed of the remaining 6 influenza genome segments originating from Luc-WSN/33 (including the luciferase-encoding segment). Known as the 6+2 reassortment strategy (Hoffmann et al., 2002), this method has the advantage of creating viruses differing only

Fig. 1. EVs demonstrate a HA-/NA-dependent inhibitory effect on influenza Quantification of viral replication of various Luc-strains. MDCK cells were co-incubated with the indicated Luc-strain (MOI = 1) and EVs (EV:cell = 2). Viral replication was quantified by luminescence readout and tracked over 16-24 h. Data represent mean luminescence AUC from individual wells normalized to mean AUC from untreated wells (dashed line) for a given Luc-strain. For each Luc-strain, significance between the mean AUC of EV-treated wells and that of untreated wells were calculated and depicted in the figure. Filled shapes and bars indicated strains determined to be sensitive to inhibition by EVs, while open shapes and bars indicate strains resistant to inhibition by EVs. n = 3 individual experiments with 6 replicates per condition per experiment. Error bars = SD.
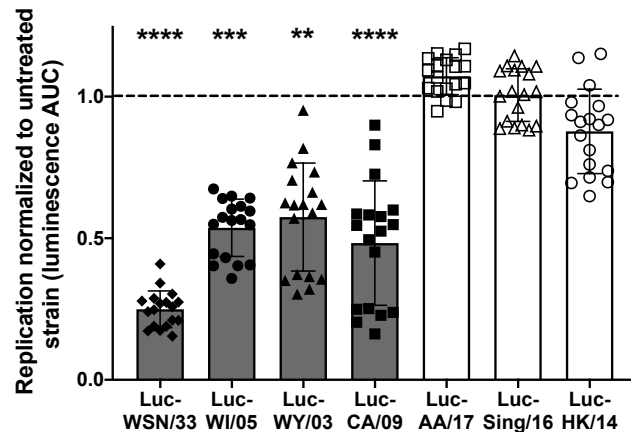
by HA and NA, which are the major sources of variability in virulence between strains (Sakai et al., 2017). Additionally, replication of these strains can be tracked using luminescence as a high-throughput readout. Schneider et al. previously measured the inhibitory effect of EVs on the Luc-HK/14 and Luc-CA/09 strains in MDCK cells using luminescence readout to quantify viral replication. These experiments showed that Luc-CA/09, but not Luc-HK/14 was inhibited by treatment of MDCK cells with EVs (Schneider et al., unpublished data). Given that these reassortant strains differ only in their expressed HA/NA, these preliminary results suggested that these surface proteins determine influenza strain sensitivity to the inhibitory effects of EVs.

To validate these findings, we generated an expanded panel of reassortant viruses derived from patient-isolated strains (Table 1). Using the same method and analysis as before, we found that Luc-expressing WSN/33, WI/05, WY/03, and CA/09 strains (filled shapes) were susceptible to inhibition by EVs, but Luc-expressing AA/17, Sing/16, and HK/14 (open shapes) strains were resistant to this inhibition (Fig. 1). As with Luc-CA/09 and HK/14, these seven strains differ only in their expressed HA/NA. Given the divergent sensitivity to inhibition by EVs displayed in this expanded panel of influenza strains, we concluded that EVs inhibit influenza replication at stage which depends on HA or NA.

EVs prevent viral-endosomal fusion and subsequent trafficking to the nucleus

To further characterize the effect of EVs on influenza, we sought to identify the stage of viral replication inhibited by EVs. Data in Fig. 1 suggested that EVs inhibit influenza infection at a stage that depends on HA or NA. Several stages of the influenza replication cycle require the proper functioning of HA and/or NA: plasma membrane binding, viral-endosomal fusion, virion assembly, and plasma membrane budding (Matsuoka et al., 2013). Additionally, data collected prior to this thesis demonstrated that EVs inhibit influenza in AECs at an intracellular stage of the viral replication cycle (Schneider et al., unpublished data). This inhibition occurs early (between 1-3 hours of infection) (Schneider et. al., unpublished data), suggesting that the later HA/NA-dependent stages of the influenza replication cycle (assembly, budding, and release) are not the targets of EVs. Taken together, these data suggest that EVs inhibit influenza at the HA-dependent stage of viral-endosomal fusion. Consistent with this, EVs have been shown to be internalized by AECs into endosomes (Schneider et al., 2017), as in other cell types (Tian et al., 2013). Therefore, this led to the hypothesis that EVs inhibit HA-dependent endosomal fusion of influenza infection.

To investigate the effect of EVs on endosomal fusion of influenza, we compared the effects of EVs on the localization of an influenza marker (influenza nucleoprotein [NP]) within late endosomes and nuclei for the representative EV-sensitive (WSN/33) and EV-resistant (HK/14) strains. A549 AECs were co-incubated with the indicated strain and EVs for 40 minutes. This time point was chosen to visualize localization of influenza within late endosomes (Qin et al., 2019). We labeled cells with primary antibodies for

Fig. 2. EVs trap influenza in late endosomes.
(A) A549 cells were co-incubated with WSN/33 or HK/14 for 40 min +/- EVs. Cells were washed, fixed, permeabilized, and stained with antibodies against influenza A NP (green) and the late endosomal marker Rab7 (magenta). Nuclei were also stained with DAPI (blue). Images shown are representative of 8 independent experiments. (B) Localization of influenza to the nucleus is represented as a ratio of the intensity of NP staining colocalized within nuclei (NP:DAPI) to the total intensity of NP staining in the cell. Colocalization of influenza to late endosomes was quantified by measuring the Manders Coefficient of the influenza marker NP with the late endosomal marker Rab7. Individual data points represent values calculated from z stack images from individual cells. n = 8 individual experiments with $\geq$ 5 z-stack images of individual cells per condition per experiment. Error bars = SD.
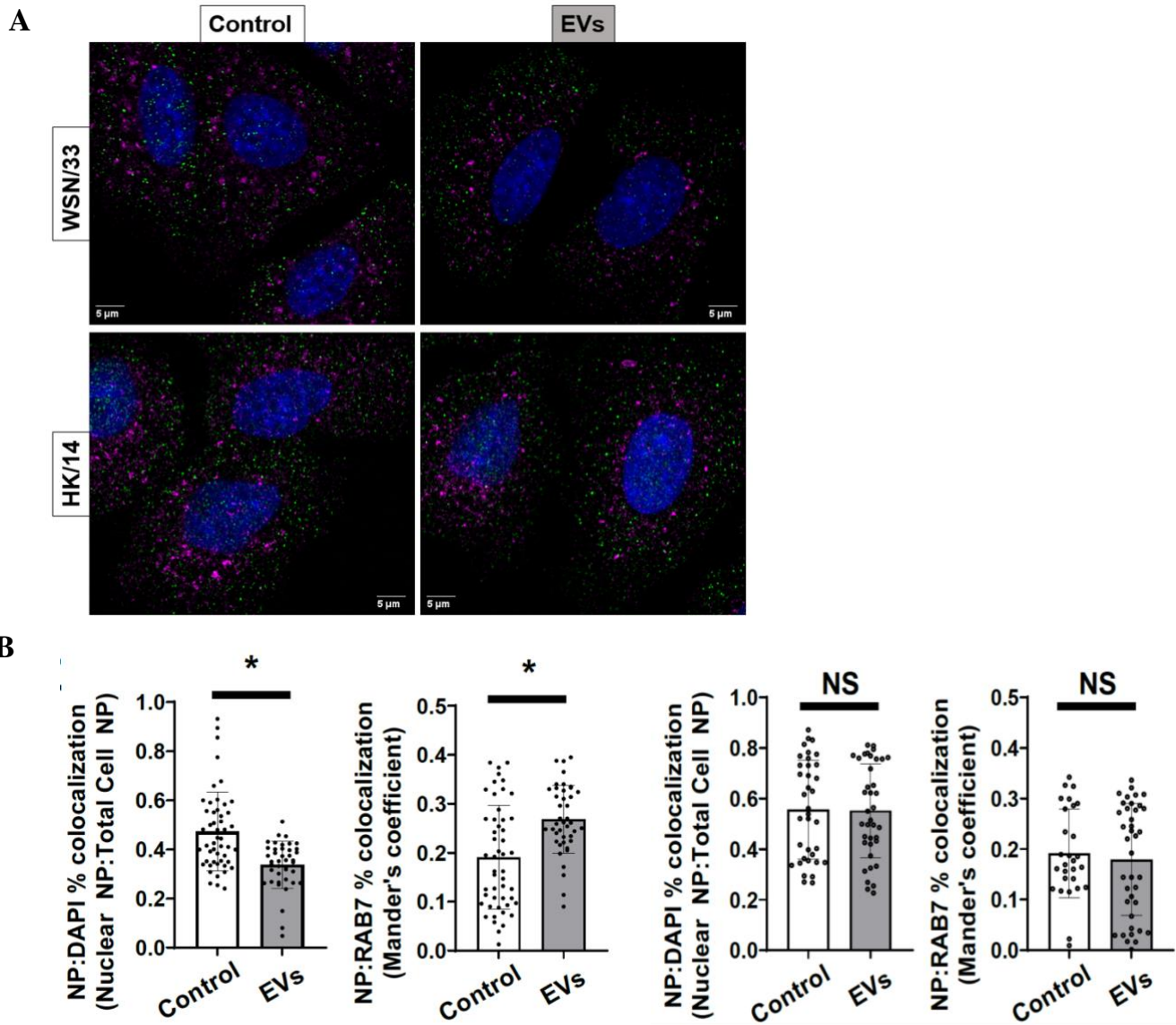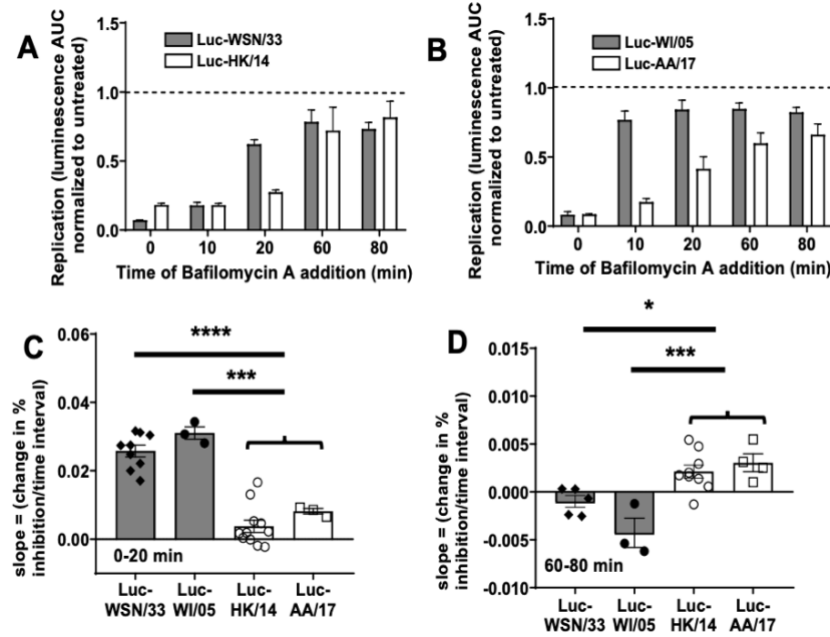
influenza A NP and Rab7, a late endosomal marker. Localization of WSN/33 NP with nuclear (DAPI) and Rab7 markers was captured by immunofluorescence microscopy. Colocalization of NP with DAPI and Rab7 markers was quantified (Fig. 2B). Influenza within late endosomes was quantified by colocalization of NP with Rab7. NP localization within DAPI was used to quantify viral escape from the endosome and subsequent nuclear trafficking. In Figs. 2A, B, we demonstrated that treatment of AECs with EVs increased endosomal colocalization of WSN/33. As anticipated, there was no significant change in endosomal colocalization of HK/14 associated with treatment with EVs (Figs. 2A, B). Consistent with these data, we demonstrated that EVs reduce detectable influenza NP within the nuclei of cells infected with WSN/33, but do not affect nuclear localization in cells infected with HK/14 (Figs. 2A, B).These results indicate that EVs inhibit replication of EV-sensitive influenza strains in AECs by prohibiting viral escape from late endosomes and subsequent trafficking to the nucleus.

Influenza strains which are resistant to inhibition by EVs are affected by acidification inhibitors at later timepoints compared to EV-sensitive strains.

Once internalized by the cell, influenza traffics within endosomes. Endosomes undergo gradual acidification as they progress from early to late endosomes (Wiley and Skehel, 1987). Acidification of the endosome triggers a conformational change in HA. This conformational change enables fusion of the viral envelope with the endosomal membrane and subsequent nuclear translocation of the virus. The pH of fusion has been suggested by several studies to be a major determinant of influenza pathogenicity (Gerlach et al., 2017; Zaraket et al., 2013), making this a puissant target for innate host defenses. Previous studies demonstrated that the pH range that enables influenza to fuse with the endosomal membrane differs for each strain (Galloway et al., 2013). Given our results and previous findings regarding an HA-determined pH of fusion, we hypothesized that EVs confine influenza to late endosomes by affecting endosomal acidification. Thus, endosomal pH would be sufficiently changed to prevent HA-dependent endosomal fusion of certain strains, but permit the fusion of other strains.

To investigate whether the differential sensitivity of influenza strains to treatment by EVs is related to differences in their pH of fusion, we characterized the dynamics of their escape from the endosome. Because endosomes undergo progressive acidification, the longer an influenza virion remains in an endosome, the lower the endosomal pH (Huotari and Helenius, 2011). Correspondingly, strains with a lower pH of fusion fuse later in endosomes (White and Whittaker, 2016). To qualify the difference in the pH of fusion of representative EV-sensitive and EV-resistant strains, we added high doses of the endosomal acidification inhibitor bafilomycin at discrete timepoints following viral internalization and tracked viral replication post-bafilomycin addition (Figs 3A, B). Because endosomes gradually acidify, viral replication post-bafilomycin addition is a readout of the virions that had already escaped from the endosome and progressed to subsequent steps of the viral replication cycle before endosomal acidification was halted. Therefore, in strains where replication is inhibited at early timepoints of bafilomycin addition, this would indicate that endosomal fusion of these strains occurs at a higher pH than strains inhibited by later timepoints of addition.

Fig. 3. Influenza strains resistant to treatment with EVs escape the endosome at earlier timepoints than strains susceptible to inhibition by EVs.

MDCK cells were pre-treated with the indicated Luc-strain on ice for 30 min to permit viral binding but prohibit internalization, washed, then brought to 37°C to permit synchronous internalization of virus at time 0. 10nM of bafilomycin were added at the indicated timepoints post-internalization and viral replication was quantified by luminescence. (A, B) 1 experiment representative of 5 individual experiments is shown for each strain. Results are expressed as mean AUC normalized to vehicle control (dashed line). (C, D) Kinetics of endosomal escape are depicted by loss of inhibition by bafilomycin. Results are expressed as the rate of viral replication relative to vehicle control from (C) 0-20 min or (D) 60-80 min post-bafilomycin addition. Data points represent mean slope (change in % inhibition/time interval) for each experiment. Bars represent the mean of each experimental average within a condition. n = 5 individual experiments with 5 replicates per viral condition per experiment. Error bars = SEM.

Fig. 4. Influenza strains resistant to treatment with EVs are inhibited by acidification inhibitors at lower doses than strains susceptible to inhibition by EVs.

Replication of various Luc-strains in MDCK cells primed and co-incubated with the indicated concentration of acidification inhibitors (A) bafilomycin or (B) chloroquine was quantified. Curves with filled shapes filled bars indicate EV-sensitive strains, while curves with open shapes and open bars indicate EV-resistant strains. AUC values were calculated and averaged among 3 replicates per condition within an individual experiment. Results represent the mean of the average AUC from individual experiments for a given condition. n ≥ 3 individual experiments. Error bars = SEM.
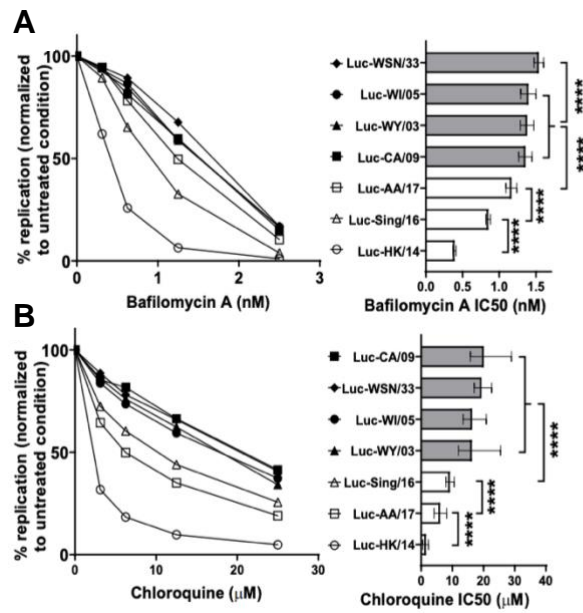
Figs. 3A, B demonstrate representative endosomal escape assays of EV-sensitive (filled bars) and EV-resistant (open bars) Luc-expressing influenza strains. As indicated by Figs. 3A, B, immediate bafilomycin addition inhibited the replication of all Luc-expressing influenza strains by at least 80%, demonstrating that all strains require some degree of endosomal acidification to escape the endosome and progress through the

replication cycle. Bafilomycin addition at and beyond 20 minutes had no ability to inhibit the replication of both EV-sensitive strains, Luc-WSN/33 and Luc-WI/05 (Figs. 3A, B), indicating that all virions had escaped the endosome within 20 min. Conversely, replication of the EV-resistant Luc-HK/14 and Luc-AA/17 was inhibited at 20 min post-internalization and continued to exhibit some level of inhibition when bafilomycin was added at 60 min, demonstrating that these strains escaped the endosome later than Luc-WSN/33 and Luc-WI/05.

The slope of the change in inhibition was also calculated in order to quantify this differential timing of endosomal escape across all experiments. As shown in Figs. 3C, D, EV-sensitive strains exhibited significantly more endosomal escape within 20 minutes post-internalization compared to EV-resistant strains. Conversely, EV-sensitive strains demonstrated no late (60-80 minutes post-internalization) endosomal escape, while EV-resistant strains continued to exhibit escape at this late timepoint. Cumulatively, these data demonstrate that EV-sensitive strains escape endosomes earlier than EV-resistant strains. This suggests that EV-sensitive strains have a higher pH of fusion than EV-resistant strains.

Influenza strains which are resistant to inhibition by EVs are sensitive to acidification inhibitors.

To more completely qualify the difference in the pH of fusion of the Luc-strains used in in Fig. 1, we investigated their sensitivity to inhibition by bafilomycin as well as an additional endosomal acidification inhibitor known as chloroquine. We hypothesized that the replication of strains with a higher pH of fusion would be inhibited at lower doses of the acidification inhibitors than strains which require a lower pH to fuse with the endosomal membrane. MDCK cells were pre-incubated for 30 mins with the indicated concentration of bafilomycin (Fig. 4A) or chloroquine (Fig. 4B). Cells were subsequently co-incubated with the indicated Luc-stain and acidification inhibitor. Replication of EV-resistant strains (open shapes and bars, Figs. 4A, B) was reduced by 50% at bafilomycin and chloroquine concentrations at or below 1.25nM and 10μM, respectively, while the inhibition of EV-sensitive strains (filled shapes and bars, Figs. 4A, B) required 1.5nM and 20uM of bafilomycin and chloroquine, respectively, to reach this level of inhibition. These results demonstrate that EV-sensitive strains require higher doses of endosomal acidification inhibitors to inhibit replication to the same extent as EV-resistant strains. Furthermore, these results support our hypothesis that the pH of fusion for EV-sensitive strains is higher than that of EV-resistant strains.

DISCUSSION

Various protective roles of AMs in influenza infection have been described, including their secretion of pro-inflammatory cytokines, ingestion of apoptotic bodies, and sequestration of the virus. However, the immobile nature and sparse concentration of AMs in the distal airways prompted the exploration of a role of AMs that had yet to be explored in the context of influenza infection: that of AM paracrine signaling via EVs. Unpublished data (Schneider et al.) which preceded the experiments in this honors

thesis demonstrated that EVs inhibited influenza at a stage in the viral replication cycle which was both intracellular and HA-/NA-dependent. This led us to hypothesize that EVs inhibit influenza replication in AECs at the HA-dependent stage of viral-endosomal fusion. In this thesis, we first confirmed preliminary results demonstrating the differential sensitivity of influenza to treatment with EVs in an expanded panel of influenza strains differing solely in HA/NA. We then sought to characterize the effect of EVs on viral-endosomal fusion by analyzing the colocalization of influenza NP with a late endosomal marker. We found that treatment of AECs with EVs increased localization of a representative EV-sensitive, but not EV-resistant, strain to late endosomes. Correspondingly, treatment with EVs prohibited a representative EV-sensitive strain from entering the nucleus. Furthermore, we characterized the effect of various doses and timed addition of acidification inhibitors on viral replication and found that the strain sensitivity to EVs closely followed trends in the different optimal pH of fusion of these strains. We concluded that EVs inhibit viral-endosomal fusion and suggest that this inhibition is a result of accelerating endosomal acidification. Taken together, our results demonstrate that EVs target a puissant step in the replication cycle of many enveloped viruses and may be an important host defense against infection by this subset of viruses.

Previous findings demonstrated an HA-dependent difference in the optimal pH of fusion of influenza strains (Galloway et al., 2014; Singanayagam et al., 2019). By characterizing the timing of endosomal escape and acidification inhibitor dose response of our various strains, our findings supported the conclusion that different strains have different pH of fusions. Furthermore, our data suggested that EV-sensitive strains require a higher pH of fusion than EV-resistant strains. The most likely explanation for these observed trends is that EVs act to decrease endosomal pH in recipient cells. Thus, it is possible that treatment of infected cells with EVs accelerates endosomal acidification such that the endosomal pH falls beneath the range tolerated for fusion of susceptible strains with the endosomal membrane. Consequently, these strains are trapped in late endosomes and likely ushered to the ultimate destination for many endosomes: lysosomal degradation. In this model, acceleration towards a lower pH would have a neutral effect on the replication of resistant strains, as was demonstrated in Fig. 1. In the hopes of validating the model suggested here, future experiments may be performed to establish pH differences in endosomes containing EVs versus those that do not contain EVs.

The pH stability of a strain's HA defines several important characteristics of a virus' replication cycle and, consequently, the course of infection. The pH stability of HA and its pH optimum of endosomal fusion have been demonstrated to be major determinants in strain-specific influenza pathogenicity (Gerlach et al., 2017), transmissibility (Zhong et al., 2014; Schrauwen and Fouchier, 2014; Russier et al., 2016), and host-specificity (Galloway et al., 2013; Zaraket et al., 2013). Strains with mutations in regions of HA critical for endosomal fusion and which lead to a higher optimal pH of fusion evade inhibition by the host antiviral interferon response more efficiently (Gerlach et al., 2017) and replicate more rapidly (Singanayagam et al., 2019). However, HA subtypes with a higher optimal pH of fusion have also been shown to undergo premature HA activation

when exposed to an acidic environment mimicking the upper respiratory tract (Singanayagam et al., 2019). Therefore, it is possible that strains with a high optimal pH of fusion have evolved to evade the interferon response. However, these strains may subsequently succumb to another layer in the host's innate immune response: the antiviral action of EVs. Importantly, it has been suggested that the high optimal pH of fusion of many avian influenzas is partly responsible for the inability of these viruses to cross to the human species effectively (Singanayagam et al., 2019). Furthermore, more epidemiologically-relevant strains, including avian and pandemic influenzas, have been shown to fuse with the endosome at higher pH values than seasonal strains (Russier et al., 2016). Because of their high pH of fusion, these strains are likely capable of circumventing the host's interferon defenses. However, our studies have demonstrated a mechanism by which the host may combat infection of AECs with these more epidemiologically-relevant strains by exploiting their relatively high pH of fusion. Thus, our study has helped illuminate the host's ability to target a subset of influenza strains which may circumvent the host's antiviral interferon response.

Previous studies suggest that EVs isolated from tracheobronchial epithelial cells prevent influenza infection of ECs by binding to influenza extracellularly through sialic acid residues on the surface of these non-AM-EVs (Kesimer et al., 2009). This thesis and its preliminary studies demonstrated a clear intracellular inhibitory action of EVs on influenza in ECs, specifically at the point of viral-endosomal fusion. The differences between the antiviral activities demonstrated in previous studies versus those demonstrated in this thesis are likely due to differences in the cell type origin of the EVs. Thus, our study in combination with that of Kesimer et al. (2009) suggests that different airway regions within the host have developed distinct innate host defenses against influenza.

While we have classified the effect of EVs on influenza infection here, there remain several unknowns regarding the source of influenza resistance imparted to AECs by EVs. For example, the molecular mediator(s) of this antiviral activity have yet to be identified. Schneider et al. has determined the source of this activity is not RNA-based and is likely one or multiple proteins or lipids. Because the responsible molecule(s) have yet to be identified, efforts to characterize a precise mechanism of action are somewhat limited. Future studies will seek to identify the mediator(s) of this activity via depletion of targeted lipid(s) and proteomic analysis. Additionally, the effect of AM infection on the cell's packaging of this antiviral molecule(s) has yet to be determined. If future studies demonstrate that infection of the AM alters its secretion of this antiviral cargo, this would suggest influenza has a possible means of combating this host defense in vivo. Identification of the antiviral molecule(s) in EVs as well an understanding of its packaging by AMs during an infection and its antiviral mechanism in the host could prove useful in the development of antiviral therapies and preemptive measures.

Currently, influenza vaccines are only 14-60% effective (CDC, 2020), and their effectiveness is dependent upon the proper identification of 3-4 strains estimated to be the most virulent in a given season and chosen as targets for the vaccine. Several vaccines employ adjuvants – ingredients used to elevate the recipient's immune

response for the purpose of improving the effectiveness of the vaccine. Currently, most influenza vaccines do not contain adjuvants (CDC, 2018). However, our discovery and characterization of a host defensive measure against influenza infection may lead to further exploration in host immunity against influenza such that addition of adjuvants to the seasonal influenza vaccine may become an obvious next step to improving preemptive measures. Furthermore, the antiviral cargo whose effects we have described here may prove useful as a treatment for not only influenza, but other relevant pathogens internalized into endosomes.

LITERATURE CITED

Asai, H., Ikezu, S., Tsunoda, S., Medalla, M., Luebke, J., Haydar, T., and T. Ikezu. 2015. Depletion of microglia and inhibition of exosome synthesis halt tau propagation. *Nature Neuroscience* 18(11): 1584-1593. doi:10.1038/nn.4132

Bhattacharya, J., and K. Westphalen. 2016. Macrophage-epithelial interactions in pulmonary alveoli. *Semin Immunopathol* 38: 461–469.

Bourdonnay, E., Zaslona, Z., Penke, L., Speth, J., Schneider, D., Przybranowski, S., Swanson, J., Mancuso, P., Freeman, C., Curtis, J., and M. Peters-Golden. (2015). Transcellular delivery of vesicular SOCS proteins from macrophages to epithelial cells blunts inflammatory signaling. *J Exp Med* 212: 729-742.

Centers for Disease Control and Prevention Foundation. 2014. *Flu Costs the U.S. More Than $87 Billion Annually.* Retrieved from https://www.cdcfoundation.org/pr/flu-costs-United-States-87-billion-annually

Centers for Disease Control and Prevention. 2017. *Influenza Type A Viruses.* Retrieved from https://www.cdc.gov/flu/avianflu/influenza-a-virus-subtypes.htm

Centers for Disease Control and Prevention. 2018. *Adjuvants help vaccines work better.* Retrieved from https://www.cdc.gov/vaccinesafety/concerns/adjuvants.html

Centers for Disease Control and Prevention. 2019. *Estimated Influenza Illnesses, Medical visits, Hospitalizations, and Deaths in the United States — 2017–2018 influenza season.* Retrieved from https://www.cdc.gov/flu/about/burden/2017-2018.htm

Centers for Disease Control and Prevention. 2020. *Vaccine Effectiveness: How Well Do the Flu Vaccines Work?* Retrieved from https://www.cdc.gov/flu/vaccines-work/vaccineeffect.htm

Cohen, M., Zhang, X., Senaati, H., Chen, H., Varki, N., Schooley, R., and P. Gagneux. 2013. Influenza A penetrates host mucus by cleaving sialic acids with neuraminidase. *Virology Journal* 10:321. doi:10.1186/1743-422X-10-321

Duan, M., Hibbs, M., and W. Chen. 2017. The contributions of lung macrophage and monocyte heterogeneity to influenza pathogenesis. *Immunol Cell Biol* 95**:** 225-235.

Elkin, S., Lakoduk, A., and S. Schmid. 2016. Endocytic pathways and endosomal trafficking: a primer. *Wien Med Wochenschr* 166**:** 196–204. doi: 10.1007/s10354-016-0432-7.

Fu, Y., Zhang, L., Zhang, F., Tang, T., Zhou, Q., Feng, C., Jin, Y., and Z. Wu. 2017. Exosome-mediated miR-146a transfer suppresses type I interferon response and facilitates EV71 infection. *PLOS Pathogens* 13(9): e1006611.

Galloway, S., Reed, M., Russell, C., and D. Steinhauer. 2013. Influenza HA Subtypes Demonstrate Divergent Phenotypes for Cleavage Action and pH of Fusion: Implication for Host Range and Adaptation. *PLoS Pathogens* 9(2).

Gerlach, T., Hensen, L., Matrosovich, T., Bergmann, J., Winkler, M., Peteranderl, C., Klenck, H., Wever, F., Herold, S., Pohlman, S., and M. Matrosovich. 2017. pH Optimum of Hemagglutinin-Mediated Membrane Fusion Determines Sensitivity of Influenza A Viruses to the Interferon-Induced Antiviral State and IFITMs. *Journal of virology* 91. doi: 10.1128/JVI.00246-17.

Goto, H., and Y. Kawaoka. 1998. A novel mechanism for the acquisition of virulence by a human influenza A virus. *Proceedings of the National Academy of Sciences* 95(17): 10224-10228. doi: 10.1073/pnas.95.17.10224

He, W., Chen, C., Mullarkey, C., Hamilton, J., and C. Wong. 2017*.* Alveolar macrophages are critical for broadly-reactive antibody-mediated protection against influenza A virus in mice. *Nat Commun* 8: 846. doi: 10.1038/s41467-017-00928-3

Hoffmann, E., Krauss, S., Perez, D., Webby, R., and R. Webster. 2002. Eight-plasmid system for rapid generation of influenza virus vaccines. *Vaccine* 20**:** 3165-70.

Huotari, J, and A. Helenius. 2011. Endosome maturation. *The EMBO journal* 30(17): 3481-500. doi:10.1038/emboj.2011.286

Speth, J., Bourdonnay, E., Raghu, L., Penke, K., Mancuso, P., Moore, B., Weinberg, J., and M. Peters-Golden. 2016. Alveolar Epithelial Cell–Derived Prostaglandin E_2 Serves as a Request Signal for Macrophage Secretion of Suppressor of Cytokine Signaling 3 during Innate Inflammation. *Journal of Immunology* 196 (12): 5112-5120. doi: 10.4049/jimmunol.1502153

Kesimer, M., Scull, M., Brighton, B., Demaria, G., Burns, K., O'Neal, W., Pickles, R., and J. Sheehan. 2009. Characterization of exosome-like vesicles released from human tracheobronchial ciliated epithelium: a possible role in innate defense. *Faseb j* 23**:** 1858-68.

Lenassi, M., Cagney, G., Liao, M., Vaupotic, T., Bartholomeeusen, K., Cheng, Y., Krogan, N., Plemenitas, A., and B. Peterlin. 2010. HIV Nef is secreted in exosomes and triggers apoptosis in bystander CD4+ T cells. *Traffic* 11(1): 110–22. pmid:19912576

Liu, Z., Zhang, X., Yu, Q., and J. He. 2014. Exosome-associated hepatitis C virus in cell cultures and patient plasma. *Biochemical and biophysical research communications* 455: 218–22. pmid:25449270.

Liu, Y., Tseng, C., Chen, Y., Yu, W., Ho, M., and C. Ho. 2019. Exosome-delivered and Y RNA-derived small RNA suppresses influenza virus replication. *J Biomed Sci* 26**.** doi: 10.1186/s12929-019-0553-6

Madison, M., and C. Okeoma. 2015. Exosomes: Implications in HIV-1 Pathogenesis. *Viruses* 7(7):4093–118. pmid: 26205405

Maemura, T., Fukuyama, S., Sugita, Y., Lopes, T.J.S., Nakao, T., Noda, T., and Y. Kawaoka. 2018. Lung-derived exosomal miR-483-3p regulates the innate immune response to influenza virus infection. *J Infect Dis* 217: 1372–1382. doi: 10.1093/infdis/jiy035

Margolis, L., and Y. Sadovsky. 2019. The biology of extracellular vesicles: The known unknowns. *PLoS Biol* 17(7): e3000363. doi: 10.1371/journal.pbio.3000363

Matsuoka, Y., Matsumae, H., Katoh, M. Eisfeld, A., Neumann, G., Hase, T., Ghosh, S., Shoemaker, J., Lopes, T., Watanabe, T., Watanabe, S., Fukuyama, S., Kitano, H. and Y. Kawaoka. 2013. A comprehensive map of the influenza A virus replication cycle. *BMC Systems Biology* 7: 97.

Meckes, D., and N. Raab-Traub. 2011. Microvesicles and Viral Infection. *J virol* 85(24): 12844-12854. doi: 10.1128/JVI.05853-11

Moldoveanu, B., Otmishi, P., Jani, P., Walker, J., Sarmiento, X., Guardiola, J., Saad, M., and J. Yu. 2009. *J Inflamm Res* 2: 1-11.

Nyirenda M, Omori R, Tessmer HL, Arimura H., and K. Ito. 2016. Estimating the Lineage Dynamics of Human Influenza B Viruses. PLoS ONE 11(11): e0166107. doi: 10.1371/journal. pone.0166107

Oslund, K., and Baumgarth, N. (2011). Influenza-induced innate immunity: regulators of viral replication, respiratory tract pathology & adaptive immunity. *Future Virol,* 6(8): 951-962.

Peters-Golden, M. 2004. The alveolar macrophage the forgotten cell in asthma. *Am J Respir Cell Mol Biol* 31: 3–7. doi: 10.1165/rcmb.f279

Qin, C., Li, W., Li, Q., Yin, W., Zhang, X., Zhang, Z., Zhang, X., and Z. Cui. 2019. Real-time dissection of dynamic uncoating of individual influenza viruses. *PNAS* 116(7): 2577-2582. doi: 10.1073/pnas.1812632116

Robbins, P., and A. Morelli. 2014. Regulation of immune responses by extracellular vesicles. *Nat Rev Immunol* 14: 195–208. doi: 10.1038/nri3622

Rubins, J. 2003. Alveolar Macrophages: Wielding the Double-Edged Sword of Inflammation. *American Journal of Respiratory and Critical Care Medicine* 167(2).

Rudnick, N., Griffey, C., Guarnieri, P., Gerbino, V., Wang, X., Piersaint, J., and T. Maniatis. 2017. Distinct roles for motor neuron autophagy early and late in the SOD1G93A mouse model of ALS. *PNAS*. doi: 10.1073/pnas.1704294114

Russier, M. Guohua, Y., Rehgb, J., Wonga, S., Mostafaa, H., Fabrizioa, T., Barmana, S., Kraussa, S., Webstera, R., Webbya, R., and C. Russell. 2016. Molecular requirements for a pandemic influenza virus: An acid-stable hemagglutinin protein." *PNAS* 113(6):1636-41. doi:10.1073/pnas.1524384113

Sakai, T., Nishimura, S., Naito, T., and M. Saito. 2017. Influenza A virus hemagglutinin and neuraminidase act as novel motile machinery. *Sci Rep* 7: 45043. doi: 10.1038/srep45043

Schneider, D., Speth, J., Penke, L., Wettlaufer, S., Swanson, J. A., and M. Peters-Golden. 2017. Mechanisms and modulation of microvesicle uptake in a model of alveolar cell communication. *J Biol Chem* 292: 20897–20910. doi: 10.1074/jbc.M117.792416

Schneider, D., Smith, K., Latuszek, C., Wilke, C., Lyons, D., Penke, L., Speth, J., Marthi, M., Swanson, J., Moore, B., Lauring, A., and Marc Peters-Golden. (2020). *Alveolar Macrophage-Derived Extracellular Vesicles Inhibit Endosomal Fusion of Influenza Virus.* Unpublished manuscript, Department of Pulmonary and Critical Care Medicine, University of Michigan, Ann Arbor, USA.

Schrauwen, E., and R. Fouchier. 2014. Host adaptation and transmission of influenza A viruses in mammals. *Emerging microbes & infections* 3(2): e9. doi:10.1038/emi.2014.9

Seo, S., Webby, R., and R. Webster. 2004. No apoptotic deaths and different levels of inductions of inflammatory cytokines in alveolar macrophages infected with influenza viruses. *Virology* 329**:** 270-9.

Shtyrya, Y., Mochalova, L., and N. Bovin. 2009. Influenza virus neuraminidase: structure and function. *Acta Naturae* 1(2):26-32.

Singanayagam, A., Zambron, M., and W. Barclay. 2019. Influenza Virus with Increased pH of Hemagglutinin Activation Has Improved Replication in Cell Culture but at the Cost of Infectivity in Human Airway Epithelium. *J Virol* 93.

Staeheli, P., Grob, R., Meier, E., Sutcliffe, J., and O. Haller. 1988. Influenza virus-susceptible mice carry Mx genes with a large deletion or a nonsense mutation. *Mol Cell Biol* 8**:** 4518-23.

Thangavel, R., and N. Bouvier. 2014. Animal models for influenza virus pathogenesis, transmission, and immunology. *J Immunol Methods* 410**:** 60-79.

Théry, C., Ostrowski, M., and E. Segura. 2009. Membrane vesicles as conveyors of immune responses. *Nat Rev Immunol* 9: 581–593. doi: 10.1038/nri2567

Tian, T., Zhu, Y., Hu, F., Wang, Y., Huang, N., and Z. Xiao. 2013. Dynamics of exosome internalization and trafficking. *J cell phys* 228. doi: 10.1002/jcp.24304.

Tran, V., Moser, L., Poole, D., and A. Mehle. 2013. Highly Sensitive Real-Time In Vivo Imaging of an Influenza Reporter Virus Reveals Dynamics of Replication and Spread. *J Virol* 87(24): 13321-13329.

Westphalen, L., Gusarova, G., Islam, M, Subramanian, M., Cohen, T., Prince, A., and J. Bhattacharya. 2014. Sessile alveolar macrophages communicate with alveolar epithelium to modulate immunity. *Nature* 506**:** 503-6.

White, J., and G. Whittaker. 2016. Fusion of Enveloped Viruses in Endosomes. *Traffic* 17(6): 593-614. doi:10.1111/tra.12389

Wiley, D., and J Skehel. 1987. The structure and function of the hemagglutinin membrane glycoprotein of influenza virus. *Annu Rev Biochem* 56: 365-94.

World Health Organization. 2020. *Virology of human influenza.* Retrieved from http://www.euro.who.int/en/health-topics/communicable-diseases/influenza/data-and-statistics/virology-of-human-influenza

Yang, X., Steukers, L., Forier, K., Xiong, R., Braeckmans, K., Reeth, K., and H. Nauwynck. 2014. A Beneficiary Role for Neuraminidase in Influenza Virus Penetration through the Respiratory Mucus. *PLoS ONE* 9(10): e110026. doi:10.1371/journal.pone.0110026

Zaraket, H., Baranovich, T., Kaplan, B., Carter, R., Song, M., Paulson, J., Rehg, J., Bahl, J., Crumpton, J., Seiler, J., Edmonson, M., Wu, G., Karlsson, E., Fabrizio, T. , Zhu, H., Guan, Y., Husain, M., Schultz-Cherry, S., Krauss, S., McBride, R., Webster, R., Govorkova, E., Zhang, J., Russel, C., and R. Webby. 2015. Mammalian adaptation of influenza A(H7N9) virus is limited by a narrow genetic bottleneck. *Nat comm* 6. doi:10.1038/ncomms7553

Zhong, L., Wang, X., Li, Q., Liu, D., Chen, H., Zhao, M., Gu, X., He, L., Liu, X., Gu, G., Peng, D., and X. Liu. 2014. Molecular mechanism of the airborne transmissibility of H9N2 avian influenza A viruses in chickens. *J virol* 88(17): 9568-78. doi:10.1128/JVI.00943-14